A theoretical analysis for the dynamic axial crushing behaviour of aluminium foam-filled hat sections

Qingchun Wang *, Zijie Fan, Liangjin Gui

State Key Laboratory of Automotive Safety and Energy, Department of Automotive Engineering, Tsinghua University, Beijing 100084, China

Abstract

A theoretical analysis was performed to predict the dynamic axial crushing behaviour of aluminium foam-filled top hat and double hat sections made from mild steel material. The deformation mode from the test results was used to create a deformation model for the theoretical analysis. According to the energy method and the superfolding element theory, the mean dynamic crushing loads of the aluminium foam-filled hat sections and the interactive effect between the aluminium foam and hat sections were theoretically predicted. The mean dynamic crushing loads and the interactive effect predicted by this theoretical analysis were in good agreement with the experimental results. The theoretical prediction results showed that the interactive effect was mainly from the aluminium foam.
© 2005 Elsevier Ltd. All rights reserved.

Keywords: Aluminium foam; Hat section; Superfolding element; Mean dynamic crushing load; Interactive effect

1. Introduction

Impact safety and weight-saving are two important design goals for energy absorbing structures in the automotive industry. Recently, many studies showed that filling thin-walled structures with aluminium foam could improve the crashworthiness of these structures. The interactive effect between the fillers and the thin-walled structures was taken as the main reason for this improvement.

Some attempts were made to predict the interactive effect. After a comprehensive experimental study on the aluminium foam-filled thin-walled circular and square columns, Hanssen et al. (1998, 1999, 2000a,b, 2001) developed some empirical formulae of the mean crushing loads for foam-filled circular and square

---

Nomenclature

$2H$	height of the superfolding element
l	column length
a, b	column width and depth
f	flange size
t	column thickness
L	perimeter of the cross section
σ_f	aluminium foam plateau stress
ε_{ep}	strain corresponding to the end of the plateau stress region
σ_0	characteristic stress
D, p	Cowper–Symonds coefficients
$P_{c,f}^D$	mean dynamic crushing load of the foam-filled column
P_c^D	mean dynamic crushing load of the non-filled column
P_f^D	dynamic crushing resistance of the aluminium foam
P_{int}^D	interactive effect
$P_{int,c}^D$	interactive effect due to the column
$P_{int,f}^D$	interactive effect due to the aluminium foam
δ_e^D	dynamic effective crushing distance
$E_{c,f}^D$	energy absorbed by foam-filled column
E_c^D	energy absorbed by the column
E_f^D	energy absorbed by the aluminium foam

columns. In his formula, Hanssen divided the mean crushing loads of the foam-filled columns into three parts: (1) mean crushing loads from the non-filled columns, (2) uni-axial resistance from the aluminium foam contained in the columns, and (3) the interactive effect due to foam filling. Since some coefficients in Hanssen's formulae were obtained by data fitting of his test results, more tests were necessary to determine whether these formulae could be used commonly. Also these predictions could only give the mean crushing loads, but no information about the change of the deformation of the foam-filled structures was provided. Based on the numerical and experimental results, Santosa and Wierzbicki (1998) and Santosa et al. (2000) gave another empirical formula. In his formula, the interactive effect was taken to be the same as the direct compressive resistance of aluminium foam.

Several works were given to predict theoretically the mean loads of foam-filled thin-walled structures. Abramowicz and Wierzbicki (1988) predicted the crushing characteristics of foam-filled square columns, and Reid et al. (1986) and Reddy and Wall (1988) calculated the crushing behaviour of foam-filled circular tubes. Their results showed that the contribution of the dissipated energy from the compressed foam was related to the volumetric strain and volume reduction of the foam.

Hat sections are common energy absorbing structures in the automotive industry. Following the method proposed by Wierzibicki and Abramowicz (1983) and Abramowicz and Wierzbicki (1989), theoretical models for the empty hat sections were given by White et al. (1999). For aluminium foam-filled hat sections subjected to static axial crushing, based on the experimental results from Wang et al. (2004), a theoretical model was developed by Song et al. (2005). In his model, the volume reduction and volumetric strain of the foam filler contained in the hat sections were calculated, and the mean crush loads of the foam-filled hat

sections were theoretically predicted. After this, the interactive effect was theoretically calculated. All the theoretical predictions agreed well with the tests.

Mostly, the structures absorbed energy under dynamic loads. Based on experimental studies on the dynamic crushing behaviour of empty hat sections, following the static theoretical models for empty hat sections developed by White et al. (1999) and for thin-walled tubes by Abramowicz and Jones (1984, 1986) and White and Jones (1999) carried out a theoretical analysis on the dynamic mean crushing loads of top hat and double hat sections. For the foam-filled hat sections, an experimental study was performed by Wang et al. (in press) to obtain the dynamic crushing behaviour of aluminium foam-filled hat sections made from mild steel material. Dynamic axial crushing tests showed that, compared to the static test results, the crashworthiness of the foam-filled hat section was improved due to the strain rate sensitivity, and the height of the superfolding element was also increased.

In this paper, the dynamic axial crushing behaviour of foam-filled hat sections was predicted theoretically. First a correction was made to the theoretical model of empty hat sections developed by White and Jones (1999), and then based on the test results of the aluminium foam-filled hat sections subjected to dynamic axial crushing, a theoretical model was created for aluminium foam-filled hat sections, and theoretical predictions for the mean dynamic crushing loads and the interactive effect of the foam-filled hat sections were made. Finally, these theoretical predictions were compared with the test results.

2. Corrections to the theoretical analysis on the dynamic crushing of empty top hat and double hat sections

To get a simple and closed-form formula for the mean dynamic crushing loads of the empty hat sections, White and Jones (1999) made a simplification, taking the superfolding element height of the empty hat sections subjected to dynamic crushing to be the same as that under the static load. The mean dynamic crushing load was obtained by the mean static crushing load times a factor related to the average strain rate. The average strain rate for an asymmetric superfolding element subjected to dynamic axial crushing was estimated by Abramowicz and Wierzbicki (1989) and used by White et al. (1999) as

$$\dot{\varepsilon}_{av} = \frac{v_i t}{4.3 H r}, \tag{1}$$

where v_i was the initial impact velocity, t was the thickness of the hat sections, $2H$ was the height of the superfolding element, and r was the rolling radius.

For a hat section with a perfectly plastic material, the total energy dissipated during the dynamic axial crushing, E_c^D, was expressed as

$$E_c^D = \left[1 + \left(\frac{\dot{\varepsilon}_{av}}{D} \right)^{1/p} \right] E_c^S, \tag{2}$$

where E_c^S was the energy dissipated during static axial crushing, and D and p were the Cowper–Symonds coefficients. So the mean dynamic crushing load P_c^D was

$$P_c^D = E_c^D / \delta_e^D = \left[1 + \left(\frac{\dot{\varepsilon}_{av}}{D} \right)^{1/p} \right] P_c^S, \tag{3}$$

where P_c^S was the mean static crushing load. Then White and Jones (1999) used the results of H and r from the static theoretical prediction to calculate the mean average strain rate, and the mean dynamic crushing load was obtained.

Since the expression of the average strain rate was related to the parameters H and r, the mean static crushing load was obtained by minimizing with respect to the parameters H and r, so the mean dynamic

crushing load should not only be obtained by the static mean load times a factor related to the average strain rate, but should follow the same procedure as the static. Here a correction was made to the formulae from White and Jones (1999).

For example, the mean dynamic crushing load for the top hat section could be expressed as

$$P_c^D = P_c^S \left[1 + \left(\frac{\dot{\varepsilon}_{av}}{D} \right)^{1/p} \right] = \frac{\sigma_0 t^2}{4} \left[17.76 \frac{r}{t} + \pi \frac{L}{H} + 9.184 \frac{H}{r} \right] \frac{2H}{\delta_e^D} \left[1 + \left(\frac{\dot{\varepsilon}_{av}}{D} \right)^{1/p} \right]. \tag{4}$$

Using Eq. (1), the mean dynamic crushing load was

$$P_c^D = t^2 \sigma_0 \left(\left[\frac{6.08r}{t} + \frac{1.08L}{H} + \frac{3.15H}{r} \right] + \left[\left(\frac{tv_i}{4.3D} \right)^{1/p} \frac{6.08}{t} H^{-\frac{1}{p}} r^{1-\frac{1}{p}} + 1.08 H^{-1-\frac{1}{p}} r^{-\frac{1}{p}} * L + 3.15 H^{1-\frac{1}{p}} r^{-1-\frac{1}{p}} \right] \right), \tag{5}$$

where σ_0 was the energy equivalent flow stress, and L was the perimeter of the cross section, which equaled $2a + 2b + 4f$.

Here the same method as the static theoretical prediction was used to obtain the results of parameters H and r. Eq. (5) was minimized with respect to the parameters H and r and equaled to zero to get the mean dynamic crushing load, which gave

$$- 1.08LH^{-2} + 3.15r^{-1} - \frac{1}{p} \left(\frac{tv_i}{4.3D} \right)^{1/p} \frac{6.08}{t} H^{-1-\frac{1}{p}} r^{1-\frac{1}{p}} - \left(1 + \frac{1}{p} \right) \left(\frac{tv_i}{4.3D} \right)^{1/p} 1.08LH^{-2-\frac{1}{p}} r^{-\frac{1}{p}}$$

$$+ 3.15 \left(1 - \frac{1}{p} \right) \left(\frac{tv_i}{4.3D} \right)^{1/p} H^{-\frac{1}{p}} r^{-1-\frac{1}{p}} = 0, \tag{6}$$

$$\frac{6.08}{t} - 3.15Hr^{-2} + \left(\frac{tv_i}{4.3D} \right)^{1/p} \left(1 - \frac{1}{p} \right) \frac{6.08}{t} H^{-\frac{1}{p}} r^{-\frac{1}{p}} - \frac{1}{p} 1.08 \left(\frac{tv_i}{4.3D} \right)^{1/p} LH^{-1-\frac{1}{p}} r^{-1-\frac{1}{p}}$$

$$- \left(1 + \frac{1}{p} \right) 3.15 \left(\frac{tv_i}{4.3D} \right)^{1/p} H^{1-\frac{1}{p}} r^{-2-\frac{1}{p}} = 0. \tag{7}$$

The results of the parameters H and r were solved with a numerical iteration method, and then the mean dynamic crushing load was obtained according to Eq. (5).

The same procedure was used to predict the mean dynamic crushing behaviour of the double hat section, and similar expressions for the mean dynamic crushing load could be obtained, except for a few coefficients that were different in each expression.

3. Theoretical analysis for foam-filled hat sections

Based on the dynamic crushing tests of the foam-filled hat sections, the following assumptions were made for the theoretical analysis:

(1) The aluminium foam was taken as isotropic, and the Poisson's ratio was zero.
(2) The effective dynamic crushing distance δ_e^D of the superfolding element for the foam-filled hat sections was still defined as 0.73 of the original height of the superfolding element.
(3) Simplified deformation models were created to calculate the volume reduction of the aluminium foam contained in the hat sections with an original height of $4H$, as shown in Fig. 1.
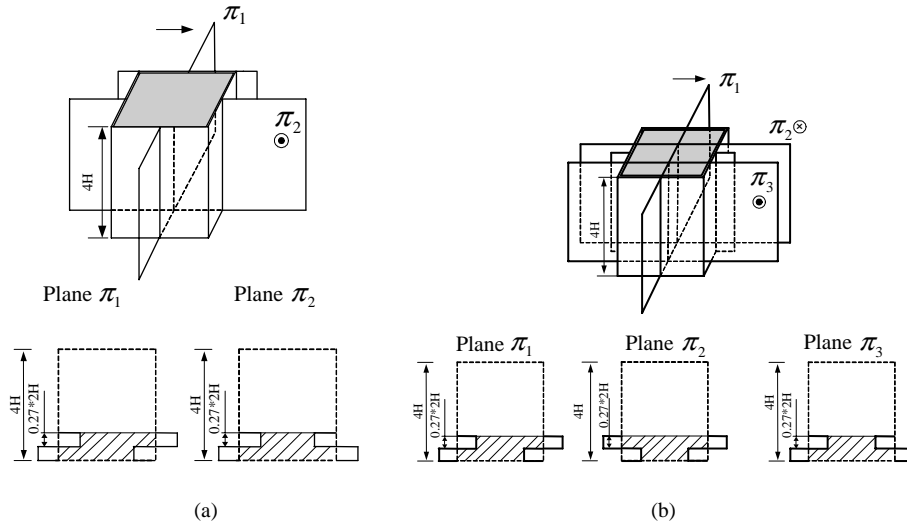
Fig. 1. Theoretical models for foam-filled hat sections. (a) Model of foam-filled top hat. (b) Model of foam-filled double hat sections.

3.1. Energy absorbed by the aluminium foam

Experimental results in Wang et al. (in press) showed that the aluminium foam was insensitive to the strain rate when the initial impact velocity was lower than 8 m/s (till 25 m/s according to Hanssen et al., 2000a). To calculate the energy dissipated in the aluminium foam, a data fit for the stress–strain relationship of aluminium foam was carried out. Here a polynomial of degree 3 was used to fit the test data after the ε_{ep} in a least-squares sense, where ε_{ep} was the strain corresponding to the end of the plateau stress region. For the stress before ε_{ep}, it was simplified as a constant plateau stress σ_f. The stress–strain curves of the test data and the fit data are shown in Fig. 2.
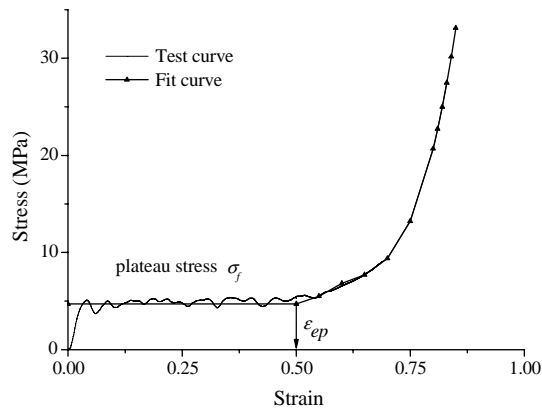

Fig. 2. Stress–strain curves of the test data and fit data.

So, the relationship between the stress and strain of the aluminium foam was written as

$$\sigma = \begin{cases} \sigma_f, & \text{when } \varepsilon \leqslant \varepsilon_{ep}, \\ \sigma_f(1 + b_3\lambda^3 + b_2\lambda^2 + b_1\lambda), & \text{when } \varepsilon > \varepsilon_{ep}, \end{cases} \tag{8}$$

where $\lambda = \varepsilon - \varepsilon_{ep}$, and b_i $(i = 1, 2, 3)$ was the coefficient of the polynomial divided by the plateau stress σ_f.

According to Fig. 1, the volume reduction of the aluminium foam contained in the hat sections with an original height of $4H$ was

$$\Delta V = (0.73H + 0.5t) \cdot (0.27 \cdot 2H + t) \cdot 2(a + b) + 4ab \cdot 0.73H$$
$$\approx 0.79(a + b)H^2 + 2Ht(a + b) + 4ab \cdot 0.73H. \tag{9}$$

The original volume of the aluminium foam in the hat sections with a height of $4H$ was $V = 4H \cdot ab$. So the total volume strain was

$$\varepsilon = \frac{\Delta V}{V} = \frac{0.79(a + b)H^2 + 4ab \cdot 0.73H + 2Ht(a + b)}{4H \cdot ab} = \varepsilon_{ep} + \frac{0.198(a + b)H}{ab} + \beta_0, \tag{10}$$

where $\beta_0 = 0.73 - \varepsilon_{ep} + (a + b)t/2ab$.

As the aluminium foam was considered an ideal isotropic material, the energy absorbed by the aluminium foam was calculated as

$$E_f^D = \int_0^\varepsilon \sigma(\varepsilon)V \, d\varepsilon$$
$$= \int_0^{\varepsilon_{ep}} 4\sigma_f abH \, d\varepsilon + \int_{\varepsilon_{ep}}^\varepsilon 4\sigma_f(1 + b_3\lambda^3 + b_2\lambda^2 + b_1\lambda)abH \, d\varepsilon \tag{11}$$
$$= 4abH\sigma_f \left(\varepsilon + \frac{b_3\lambda^4}{4} + \frac{b_2\lambda^3}{3} + \frac{b_1\lambda^2}{2} \right).$$

3.2. Mean dynamic crushing loads of foam-filled columns

Based on the above, the total energy dissipated in the formation of a foam-filled superfolding element with an original height of $4H$ was

$$E_{c,f}^D = E_c^D + E_f^D$$
$$= \sigma_0 t^2 H \left[\frac{24.33r}{t} + \frac{1.37\pi L}{H} + \frac{12.58H}{r} \right] \left[1 + \left(\frac{\dot{\varepsilon}_{av}}{D} \right)^{1/p} \right] + 4abH\sigma_f \left(\varepsilon + \frac{b_3\lambda^4}{4} + \frac{b_2\lambda^3}{3} + \frac{b_1\lambda^2}{2} \right) \tag{12}$$

and the mean dynamic crushing load was calculated as

$$P_{c,f}^D = E_{c,f}^D / \delta_e^D. \tag{13}$$

From Eqs. (12) and (13), the following expression was obtained:

$$P_{c,f}^D = K_0 + K_1 H^4 + K_2 H^3 + K_3 H^2 + K_4 H + K_5 r + K_6/H + K_7 H/r + K_8 H^{-\frac{1}{p}} r^{1-\frac{1}{p}} + K_9 H^{-1-\frac{1}{p}} r^{-\frac{1}{p}}$$
$$+ K_{10} H^{1-\frac{1}{p}} r^{-1-\frac{1}{p}}, \tag{14}$$

where K_i represented the corresponding coefficient (see Appendix A).

Eq. (14) was minimized with respect to the parameters H and r to obtain the mean dynamic crushing load, which finally gave

$$K_5 - K_7 H r^{-2} + \left(1 - \frac{1}{p}\right) K_8 H^{-\frac{1}{p}} r^{-\frac{1}{p}} - \frac{1}{p} K_9 H^{-1-\frac{1}{p}} r^{-1-\frac{1}{p}} - \left(1 + \frac{1}{p}\right) K_{10} H^{1-\frac{1}{p}} r^{-2-\frac{1}{p}} = 0, \tag{15}$$

$$4K_1 H^3 + 3K_2 H^2 + 2K_3 H + K_4 - K_6 H^{-2} + K_7 r^{-1} - \frac{1}{p} K_8 H^{-1-\frac{1}{p}} r^{1-\frac{1}{p}} - \left(1 + \frac{1}{p}\right) K_9 H^{-2-\frac{1}{p}} r^{-\frac{1}{p}}$$

$$+ \left(1 - \frac{1}{p}\right) K_{10} H^{-\frac{1}{p}} r^{-1-\frac{1}{p}} = 0. \tag{16}$$

The results of the parameters H and r were solved by a numerical iteration method, and then the mean dynamic crushing load was predicted according to Eq. (14).

4. Validation and discussion

4.1. Validation with the test results

The theoretical predictions and test results (Wang et al., in press) of the mean dynamic crushing loads for the non-filled hat sections are listed in Table 1. Here the coefficients D and p for the column material were 6844 and 3.91 respectively. For the non-filled hat sections, the theoretical results according to the formulae developed by White and Jones (1999) are also presented in Table 1. The results showed that the theoretical predictions in this paper for the mean dynamic crushing load were quite close to the predictions obtained with the method by White and Jones (1999). Both predictions agreed well with the test results. The theory developed in this paper predicted that the height of the superfolding element increased during dynamic axial crushing compared with predictions for the static crushing, which was verified by the experimental results, but the theory developed by White and Jones (1999) was not able to predict this change in deformation.

The theoretical predictions on the mean dynamic crushing loads of the aluminium foam-filled hat sections are listed in Table 2. These predictions were in good agreement with the experimental results. The theoretical results for the height of the superfolding element decreased after foam filling, just as the experimental results showed. All these comparisons showed that this theory predicted the dynamic crushing behaviour of the aluminium foam-filled hat sections quite reasonably. For mild steel, another pair of coefficients $D = 40$ and $p = 5$ is used quite often. The sensitivity of parameters H and r to the variations in coefficients D and p is shown in Table 3. From Table 3, a small change of parameters H and r was found when the coefficients D and p changed, but the mean crushing loads changed greatly.

4.2. Interactive effect

Hanssen et al. (2000a,b) divided the mean crushing loads of the foam-filled square and circular tubes into three parts:

$$P_{c,f}^D = P_c^D + \sigma_f A + P_{int}^D, \tag{17}$$

Table 1
Test results and predictions from this paper and White and Jones (1999)

	Test	Prediction by White			Prediction from this article		
	$P_{c,f}^D$ (kN)	$P_{c,f}^D$ (kN)	H (mm)	r (mm)	$P_{c,f}^D$ (kN)	H (mm)	r (mm)
SED	47.2	51.1	18.3	3.8	51.7	21.4	4.5
DED	79.4	84.2	11.5	3.0	85.2	13.8	3.7

Table 2
Test results and theoretical predictions

Sample	σ_f (MPa)	Test results		Theoretical predictions				
		$P_{c,f}^D$ (kN)	P_{int}^D (kN)	$P_{c,f}^D$ (kN)	P_{int}^D (kN)	$P_{int,f}^D$ (kN)	$P_{int,c}^D$ (kN)	H (kN)
SF1D	1.8	61.6	9.9	66.7	10.5	8.0	2.5	13.9
SF2D	2.8	68.5	12.6	70.0	11.3	8.7	2.6	13.8
SF3D	4.8	82.5	23.3	82.8	19.0	14.5	4.5	12.2
DF1D	1.8	92.0	8.1	96.9	7.2	6.4	0.8	11.3
DF2D	2.8	97.1	10.7	100.0	7.8	7.0	0.8	11.2
DF3D	4.8	108.4	17.0	111.4	14.1	12.3	1.8	10.3

Table 3
Sensitivity of H and r to D and p

Sample	$D = 6844$, $p = 3.91$			$D = 40$, $p = 5$		
	P	H	r	P	H	r
DF	111.4	10.25	3.13	165.1	12.06	3.58
DE	58.7	12.78	3.18	94.5	16.03	3.01
SF	82.8	12.14	3.46	116.0	13.92	3.95
SE	51.6	21.44	4.5	81.2	26.65	4.32

where A was the section area of the tube. Here a similar method was used for the foam-filled hat sections; the interactive effect of the foam-filled hat sections was calculated for the test results and theoretical predictions, as listed in Table 2. From the results in Table 2, it was clear that the theoretical predictions for the interactive effect agreed reasonably with the test results, proving that this theoretical analysis could be used to predict the interactive effect.

From this dynamic axial crushing theoretical model, a clear understanding of the interactive effect could be achieved. Some researchers defined $a^2\sigma_f$ as the uni-axial crush resistance of aluminium foam. But in fact this was not all the resistance that was provided by the aluminium foam. This would be true only if the aluminium foam were compressed at 50% strain. Actually, in the axial compression of the foam-filled hat sections, the final strain of the aluminium foam was greater than 0.73 (since the effective dynamic crushing distance was assumed to be 0.73 of the original superfolding element height). After the plateau region, there was a sharp increase of the stress in the mechanical characteristics of the aluminium foam. The energy absorbed in this part should be taken into account, since this was a significant contribution to the interactive effect, as illustrated by the darkened area in Fig. 3. Some contribution was from the column due to the change of H and r.

After foam filling, the values of parameters H and r were changed. P_{c1}^D could be calculated with this H and r according to Eq. (5). So the contribution from the column and foam to the interactive effect could be calculated with the following equations respectively:

$$P_{int,c}^D = P_{c1}^D - P_c^D, \tag{18}$$

$$P_{int,f}^D = P_{int}^D - P_{int,c}^D. \tag{19}$$

Calculation results based on Eqs. (18) and (19) are listed in Table 2. These results showed that the contribution of the aluminium foam to the interactive effect was much greater than that from the column.

To show some more about the contributions of the column and the aluminium foam to the interactive effect of aluminium foam-filled hat sections, the interactive effect of double hat sections filled with aluminium foam with a plateau stress of 4.8 MPa was calculated for different column thicknesses, and the results
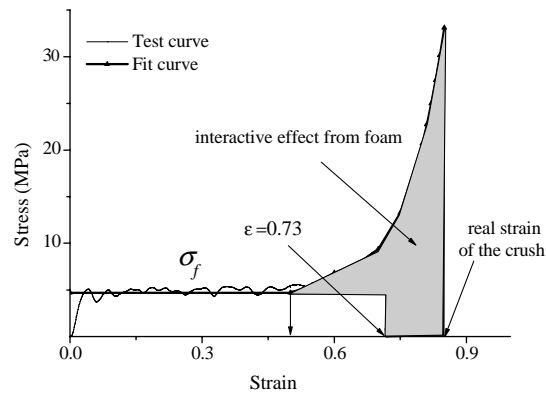
Fig. 3. Interactive effect due to aluminium foam.

Table 4
Contribution to the interactive effect

t (mm)	$P_{int,f}^D$ (kN)	$P_{int,c}^D$ (kN)	P_{int}^D (kN)
1.0	9.5	1.4	10.9
1.1	10.1	1.4	11.5
1.2	10.5	1.7	12.2
1.3	11.2	1.7	12.9
1.4	11.7	1.9	13.6
1.5	12.3	1.9	14.2
1.6	13.0	2.1	15.1
1.7	13.5	2.2	15.7
1.8	14.1	2.4	16.5
1.9	14.8	2.5	17.3
2.0	15.5	2.5	18.0

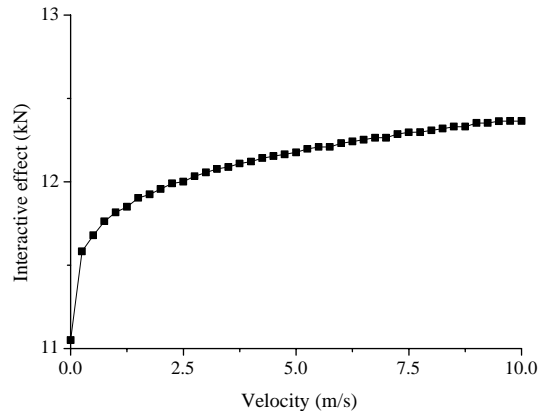Fig. 4. Relationship between interactive effect and column thickness.

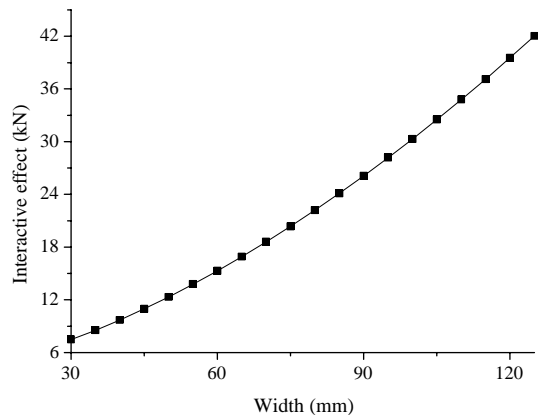Fig. 5. Relationship between interactive effect and initial velocity.

Fig. 6. Relationship between interactive effect and column width.

are listed in Table 4. The relationship between the interactive effect and the thickness for such foam-filled double hat sections are plotted in Fig. 4. Table 4 shows that the contribution from the aluminium foam governed the interactive effect, and a small contribution (less than 20%) was from the columns after the changes in the H and r.

Furthermore the effect of the initial impact velocities and the column widths on the interactive effect was calculated, and the results are presented in Figs. 5 and 6.

These figures showed that the column width had a great impact on the interactive effect, and the initial velocity had the least effect.

5. Conclusions

A theoretical analysis was carried out to predict the mean dynamic crushing load and the interactive effect of aluminium foam-filled hat sections. Predictions from this theory for foam-filled top hat and double hat sections were in good agreement with test results. The following conclusions were drawn from this theoretical analysis:

(1) The interactive effect came mainly from the deformation of the aluminium foam; it was due to the stress–strain characteristics of the aluminium foam itself. Filled with aluminium foam, the mean dynamic crushing load of the column itself increased slightly due to the changes in the H and r.

(2) The theoretical analysis correctly predicted the reduction in the height of the superfolding element with foam filling after axial dynamic crushing compared to the non-filled.

Acknowledgement

Appendix A

λ was expressed as follows:

$$\lambda = \varepsilon - \varepsilon_{ep} = \lambda_1 H + \beta. \tag{a0}$$

The coefficients for the top hat sections were

$$K_0 = ab\sigma_f * [1 + 0.34 b_3 \beta^4 + 0.46 b_2 \beta^3 + 0.69 b_1 \beta^2], \tag{a1}$$

$$K_1 = 0.34 ab\sigma_f b_3 * \lambda_1^4, \tag{a2}$$

$$K_2 = ab\sigma_f \lambda_1^3 * [1.37 b_3 \beta + 0.46 b_2], \tag{a3}$$

$$K_3 = ab\sigma_f \lambda_1^2 * (2.05 b_3 \beta^2 + 1.37 b_2 \beta + 0.69 b_1), \tag{a4}$$

$$K_4 = 1.37 ab\sigma_f \lambda_1 (1 + b_3 \beta^3 + b_2 \beta^2 + b_1 \beta), \tag{a5}$$

$$K_5 = 6.08 k\sigma_f t, \tag{a6}$$

$$K_6 = 1.08 L t^2 k\sigma_f, \tag{a7}$$

$$K_7 = 3.15 t^2 k\sigma_f, \tag{a8}$$

$$K_8 = 6.08 k\sigma_f t \left(\frac{t v_i}{4.3D}\right)^{1/p}, \tag{a9}$$

$$K_9 = 1.08 k\sigma_f \left(\frac{t v_i}{4.3D}\right)^{1/p} L t^2, \tag{a10}$$

$$K_{10} = 3.15 k\sigma_f \left(\frac{t v_i}{4.3D}\right)^{1/p} t^2. \tag{a11}$$

For the double hat sections, coefficients K_5, K_7, K_8, and K_{10} were doubled.

References

Abramowicz, W., Jones, N., 1984. Dynamic axial crushing of square tubes. International Journal of Impact Engineering 2 (2), 170–208.

Abramowicz, W., Jones, N., 1986. Dynamic progressive buckling of circular and square tubes. International Journal of Impact Engineering 4 (4), 243–270.

Abramowicz, W., Wierzbicki, T., 1988. Axial crushing of foam-filled columns. Journal of Mechanical Mechanics 30 (3,4), 263–271.

Abramowicz, W., Wierzbicki, T., 1989. Axial crushing of multicorner sheet metal columns. Journal of Applied Mechanics 56, 113–120.

Hanssen, A.G., Langseth, M., Hopperstad, O.S., 1998. Crushing of square aluminium extrusions with aluminium foam filler—numerical analyses. SUSI Conference Proceedings: Structures under shock and impact V. ISBN 1853125903, Thessaaloniki, Greece, pp. 24–26.

Hanssen, A.G., Langseth, M., Hopperstad, O.S., 1999. Static crushing of square aluminium extrusions with aluminium foam filler. International Journal of Mechanical Sciences 41 (8), 967–993.

Hanssen, A.G., Langseth, M., Hopperstad, O.S., 2000a. Static and dynamic crushing of square aluminium extrusions with aluminium foam filler. International Journal of Impact Engineering 24 (4), 347–383.

Hanssen, A.G., Langseth, M., Hopperstad, O.S., 2000b. Static and dynamic crushing of circular aluminium extrusions with aluminium foam filler. International Journal of Impact Engineering 24 (5), 475–507.

Hanssen, A.G., Langseth, M., Hopperstad, O.S., 2001. Optimum design for energy absorption of square aluminium columns with aluminium foam filler. International Journal of Mechanical Sciences 43 (1), 153–176.

Reddy, T., Wall, R., 1988. Axial compression of foam-filled thin-walled circular tubes. International Journal of Impact Engineering 30 (7), 151–166.

Reid, S.R., Reddy, T.Y., Gray, M.D, 1986. Static and dynamic axial crushing of foam-filled sheet metal tubes. International Journal of Mechanical Sciences 28 (5), 295–322.

Santosa, S.P., Wierzbicki, T., 1998. Crash behaviour of box columns filled with aluminium honeycomb or foam. Computers & Structures 68 (4), 343–368.

Santosa, S.P., Wierzbicki, T., Hanssen, A.G., Longseth, M., 2000. Experimental and numerical studies of foam-filled sections. International Journal of Impact Engineering 24 (5), 509–534.

Song, H.W., Fan, Z.J., Gang, Y., Wang, Q.C., Tobota, A., 2005. Partition energy absorption of axially crushed aluminium foam-filled hat sections. International Journal of Solids and Structures 42 (9–10), 2575–2600.

Wang, Q.C., Fan, Z.J., Song, H.W., et al., 2004. Axial compression crush behaviour of aluminum foam-filled hat sections. Chinese Journal of Mechanical Engineering 40 (11), 98–102 (Chinese version).

Wang, Q.C., Fan, Z.J., Gui, L.J., et al., in press. Experimental studies on the crash behaviour of aluminium foam-filled hat sections. Chinese Journal of Mechanical Engineering (Chinese version).

White, M.D., Jones, N., 1999. A theoretical analysis for the dynamic axial crushing of top-hat and double-hat thin-walled sections. Proceedings of the Institution of Mechanical Engineering, Part D: Journal of Automobile Engineering 213 (D4), 307–325.

White, M.D., Jones, N., Abramowicz, W., 1999. A theoretical analysis for the quasi-static axial crushing of top-hat and double-hat thin-walled sections. International Journal of Mechanical Sciences 41 (2), 209–233.

Wierzibicki, T., Abramowicz, W., 1983. On the crushing mechanics of thin-walled structures. Journal of Applied Mechanics 50, 727–734.